American Mineralogist, Volume 106, pages 174–179, 2021

Jasonsmithite, a new phosphate mineral with a complex microporous framework, from the Foote mine, North Carolina, U.S.A.

Anthony R. Kampf[1,*,†], Aaron J. Celestian[1], and Barbara P. Nash[2]

[1]Mineral Sciences Department, Natural History Museum of Los Angeles County, 900 Exposition Boulevard, Los Angeles, California 90007, U.S.A.
[2]Department of Geology and Geophysics, University of Utah, Salt Lake City, Utah 84112, U.S.A.

Abstract

Jasonsmithite (IMA2019-121), $Mn_4^{2+}ZnAl(PO_4)_4(OH)(H_2O)_7 \cdot 3.5H_2O$, is a pegmatite-phosphate mineral from the Foote Lithium Company mine, Kings Mountain district, Cleveland County, North Carolina, U.S.A. It is interpreted as having formed by late-stage, low-temperature hydrothermal alteration. Crystals are colorless to light brown, slightly flattened prisms to about 1 mm in length with wedge-shaped terminations. The mineral is transparent with vitreous luster, white streak, Mohs hardness 2, brittle tenacity, irregular fracture, and perfect {001} cleavage. The density is 2.63(2) g/cm^3. Jasonsmithite is biaxial (–), with $\alpha = 1.561(2)$, $\beta = 1.580(2)$, $\gamma = 1.581(2)$, measured in white light. The $2V$ is 25(5)° and dispersion is $r < v$ moderate. The optical orientation is $Y = \mathbf{b}$, $X \wedge \mathbf{c} = 18°$ in obtuse β. The Raman spectrum is dominated by vibrational modes of PO_4 and ZnO_4 tetrahedra, AlO_6 and MnO_6 octahedra, and OH groups. Electron microprobe analyses gave the empirical formula $(Mn_{3.09}Fe_{0.87})_{\Sigma 3.96}Zn_{1.05}Al_{0.98}(PO_4)_4(OH)(H_2O)_7 \cdot 3.5H_2O$. The mineral is monoclinic, $P2_1/c$, $a = 8.5822(3)$, $b = 13.1770(6)$, $c = 20.3040(14)$ Å, $\beta = 98.485(7)°$, $V = 2271.0(2)$ Å^3, and $Z = 4$. The structure ($R_1 = 0.0443$ for 3685 $I > 2\sigma I$ reflections) contains zigzag chains of edge-sharing MnO_6 octahedra that corner-link to adjacent chains and to PO_4 tetrahedra to form sheets, which are decorated by ZnO_4 tetrahedra. The sheets are linked to one another via dimers of AlO_6 octahedra, forming a framework with large channels containing H_2O groups. With H_2O groups removed, the framework has a void space of 70.2% per unit cell, and a framework density of 14.5 polyhedral atoms/1000 Å^3, which would place jasonsmithite among the most porous minerals.

Keywords: Jasonsmithite, new mineral, phosphate, microporous framework structure, Raman spectroscopy, Foote mine, Kings Mountain, North Carolina, U.S.A.; Microporous Materials: Crystal-Chemistry, Properties, and Utilizations

Introduction

The Foote Lithium Company mine in the Kings Mountain district, Cleveland County, North Carolina (U.S.A.), exploits spodumene-bearing pegmatites that have yielded a wide variety of rare silicate and phosphate minerals, among them 14 new mineral species (https://www.mindat.org/loc-3280.html). Herein, we describe jasonsmithite, the fifteenth new mineral from the Foote mine.

The mineral is named "jasonsmithite" in honor of American mineral collector Jason B. Smith (b. 1977) of Charlotte, North Carolina, U.S.A. Jason has long specialized in the minerals of the Foote Lithium Company mine, where he has collected extensively. He is responsible for the discovery of the new Foote–mine mineral species fanfaniite, ferraioloite, footemineite, and kayrobertsonite, as well as for jasonsmithite. Jason Smith has given permission for this mineral to be named in his honor.

The new mineral and name have been approved by the Commission on New Minerals, Nomenclature and Classification of the International Mineralogical Association (IMA2019-121). The holotype and two cotype specimens are deposited in the collections of the Mineral Sciences Department, Natural History Museum of Los Angeles County, 900 Exposition Boulevard, Los Angeles, California 90007, U.S.A., catalog numbers 74374 (holotype), 74375 (cotype), and 74376 (cotype).

Occurrence

Jasonsmithite was found by Jason B. Smith on the East dump of the Foote Lithium Company mine, Kings Mountain district, Cleveland County, North Carolina, U.S.A. (35°12′40″N, 81°21′20″W). A brief summary of the history and geology of the Foote mine was provided by Rakovan et al. (2016). Jasonsmithite was found in solution fractures and small vugs of partially oxidized pegmatite. The pegmatite matrix consists of albite, columbite-(Fe), ferrisicklerite, fluorapatite, muscovite, quartz, sphalerite, and spodumene. The secondary association found in vugs with jasonsmithite includes eosphorite, hureaulite, jahnsite-(MnMnMn), kastningite, mangangordonite, metaswitzerite, nizamoffite, stewartite, variscite, and whiteite-(CaMnMn). Jasonsmithite is interpreted as having formed by late-stage, low-temperature hydrothermal alteration. The order of formation of secondary phases at the Foote mine typically follows a trend defined by lowering temperature and concomitant in-

* E-mail: akampf@nhm.org. ORCID 0000-0001-8084-2563
† Special collection papers can be found online at http://www.minsocam.org/MSA/AmMin/special-collections.html.

0003-004X/21/0002–174$05.00/DOI: https://doi.org/10.2138/am-2020-7582

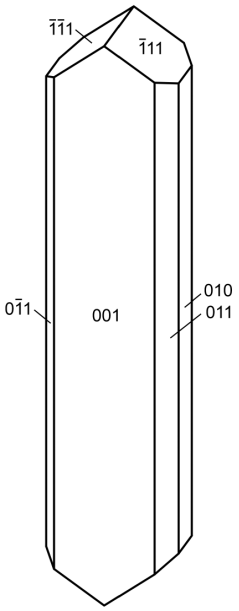

Figure 1. Crystal drawing of jasonsmithite; clinographic projection in non-standard orientation (**a** vertical).

creasing degree of hydration. For the jasonsmithite association, the order from early to late is interpreted as: (1) eosphorite; (2) hureaulite; (3) nizamoffite; (4) metaswitzerite + jasonsmithite + mangangordonite + kastningite + whiteite-(CaMnMn); (5) jahnsite-(MnMnMn) + stewartite + variscite.

Physical and optical properties

Jasonsmithite crystals are slightly flattened prisms to about 1 mm in length with wedge-shaped terminations. Elongation is parallel to [100] and flattening is on {001}. The crystal forms are {010}, {001}, {011}, and {$11\bar{1}$} (Fig. 1). Crystals commonly occur in subparallel intergrowths (Fig. 2). No twinning was observed. The color of prisms commonly varies from colorless to light brown with indistinct color boundaries (Fig. 2). The cause of the color has not been determined, although the appearance is what might be expected from indistinct submicroscopic inclusions. No compositional variation that can be correlated with the color variation was observed in the electron-probe microanalyses.

Figure 2. Jasonsmithite on holotype specimen (LACMNH 74374); FOV 0.84 mm across. (Color online.)

The streak is white, the luster is vitreous, and crystals are transparent. The mineral does not fluoresce under long- or short-wave ultraviolet light. The Mohs hardness is about 2 based on scratch tests. The tenacity is brittle, cleavage is perfect on {001}, and the fracture is irregular. The density measured by flotation in methylene iodide–toluene is 2.63(2) g/cm^3. The calculated density is 2.630 g/cm^3 for the empirical formula and 2.627 g/cm^3 for the ideal formula. At room temperature, the mineral is easily soluble in dilute HCl.

Optically, the mineral is biaxial (–), with α = 1.561(2), β = 1.580(2), γ = 1.581(2), measured in white light. The $2V$ was estimated as 25(5)° from conoscopic observation. The calculated $2V$ is 25.6° Dispersion is $r < v$ moderate. The optical orientation is Y = **b**, X ^ **c** = 18° in the obtuse angle β. No pleochroism was observed.

Raman spectroscopy

Raman spectroscopy was done on a Horiba XploRa+ micro-Raman spectrometer using an incident wavelength of 532 nm, laser slit of 50 µm, 2400 gr/mm diffraction grating, and a 100× (0.9 NA) objective. The spectrum was recorded from 4000 to 60 cm^{-1}. It was featureless between 2500 and 1200 cm^{-1}. The spectrum from 4000 to 2500 cm^{-1} is shown as an insert in the spectrum from 1200 to 60 cm^{-1} in Figure 3. A list of the band positions, half-width at half maximum intensity (HWHM), and integrated intensities are on deposit as Online Material[1] Table OM1.

The Raman spectrum of jasonsmithite is dominated by vibrational modes of the PO_4 and ZnO_4 tetrahedra, the AlO_6 and MnO_6 octahedra, and the OH groups. The OH stretching associated with H_2O and OH groups is dominant above 2200 cm^{-1} (see Fig. 3 insert). The lack of any apparent band around 1630 cm^{-1} corresponding to H_2O bending could be related to the existence

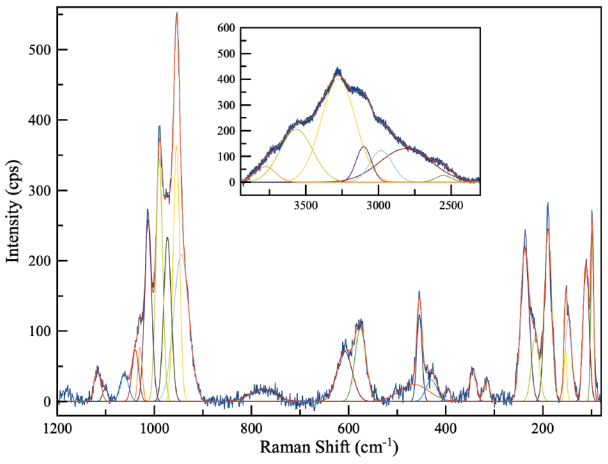

Figure 3. Background-corrected Raman spectrum of jasonsmithite recorded using a 532 nm laser. The recorded spectrum is in dark blue; the fitted bands are in various colors; the sum of the fitted bands is in red. (Color online.)

of many different H_2O sites (both on the framework and in the channel). These are likely to result in many overlapping, broad low-intensity peaks, which we do not have the resolution to observe, especially considering the high-background fluorescence in that region.

The stretching modes for the PO_4 and ZnO_4 overlap in the region at approximately 1050 to 900 cm^{-1}. Bending modes for PO_4 and ZnO_4, as well as the stretching modes for the AlO_6 and MnO_6 groups are approximately located in the 700–400 cm^{-1} region. Below 400 cm^{-1} is dominated by octahedral bending vibrations and lattice vibrations. Because of the complexity of the crystal structure, including the number of different polyhedral components within the structure and the varying local geometry of those components, it is not possible at this time to identify the precise vibrational mode for each peak in the Raman spectrum.

Chemical composition

Analyses (14 points on 2 crystals) were performed at the University of Utah on a Cameca SX-50 electron microprobe with four wavelength dispersive spectrometers and using Probe for EPMA software. Analytical conditions were 15 kV accelerating voltage, 10 nA beam current, and a beam diameter of 10 μm. Raw X-ray intensities were corrected for matrix effects with a φρ(z) algorithm (Pouchou and Pichoir 1991); total oxygen, including H_2O, was used in matrix corections. No other elements were detected by EDS or WDS wave scans. There was only minor damage from the electron beam. Because insufficient material is available for a direct determination of H_2O, it has been calculated based upon the structure determination (P = 4 and O = 27.5 apfu). The analytical results are provided in Table 1.

The empirical formula (based on 4 P and 27.5 O apfu) is $(Mn_{3.09}Fe_{0.87})_{\Sigma 3.96}Zn_{1.05}Al_{0.98}(PO_4)_4(OH)(H_2O)_7 \cdot 3.5H_2O$ (+0.05 H for charge balance). The simplified formula is $(Mn^{2+},Fe^{2+})_4ZnAl(PO_4)_4(OH)(H_2O)_7 \cdot 3.5H_2O$. The ideal formula is $Mn^{2+}_4ZnAl(PO_4)_4(OH)(H_2O)_7 \cdot 3.5H_2O$, which requires MnO 31.59, ZnO 9.06, Al_2O_3 5.68, P_2O_5 31.61, H_2O 22.06, total 100 wt%.

The Gladstone-Dale compatibility index $1 - (K_P/K_C)$ for the empirical formula is –0.010 indicating superior compatibility among the average index of refraction, calculated density, and chemical composition (Mandarino 2007).

X-ray crystallography and structure determination

Powder X-ray studies were done using a Rigaku R-Axis Rapid II curved imaging plate microdiffractometer, with monochromatized Mo*K*α radiation (λ = 0.71075 Å). A Gandolfi-like motion on the φ and ω axes was used to randomize the samples. Observed *d* values and intensities were derived by profile fitting using JADE 2010 software (Materials Data, Inc. Livermore, California). Data are given in Online Material[1] Table OM1. The observed powder diffraction pattern compares very well with the pattern calculated from the crystal structure (Fig. 4). Unit-cell parameters refined from the powder data using JADE 2010 with whole pattern fitting are $a = 8.574(5)$, $b = 13.168(5)$, $c = 20.387(5)$ Å, $\beta = 98.577(13)°$, and $V = 2276.0(17)$ Å^3.

Single-crystal data were collected using the same diffractometer and radiation noted above. The Rigaku CrystalClear software package was used for processing the structure data, including the application of an empirical absorption correction using the multi-scan method with ABSCOR (Higashi 2001). The structure was solved by the charge-flipping method using SHELXT (Sheldrick 2015a). Refinement proceeded by full-matrix least-squares on F^2 using SHELXL-2016 (Sheldrick 2015b). A difference Fourier synthesis located most H atom positions, which were then refined with soft restraints of 0.82(3) Å on the O-H distances and 1.30(3) Å on the H-H distances and with the U_{eq} of each H set to 1.2× that of the donor O atom. The crystallographic data can be found in the original CIF (as Online Material[1]). Selected bond distances are given in Table 2 and a bond-valence analysis in Table 3.

Table 1. Chemical composition (wt%) for jasonsmithite

Constituent	Mean	Range	SD	Standard
MnO	25.09	23.99–26.69	0.83	rhodonite
FeO	7.17	5.89–8.03	0.80	hematite
ZnO	9.75	8.69–10.72	0.68	syn. ZnO
Al_2O_3	5.69	5.59–5.80	0.06	sanidine
P_2O_5	32.48	31.58–33.18	0.54	apatite
H_2O[a]	22.72			
Total	102.90			

[a] Based on the structure.

Attempts to refine the occupancies of the cation sites suggested full occupancies of the Mn^{2+} sites (Mn1, Mn2, Mn3, and Mn4) by Mn, the Zn site by Zn, and the Al site by Al. The scattering powers of Mn and Fe are too similar to provide a meaningful indication of preferential occupancy of Fe in any of the Mn sites; however, the high BVS for the Mn3 site of 2.12 valence units (v.u.) suggests that Fe^{2+} is likely to prefer this site. The BVS for this site with occupancy only by Fe^{2+} is only 1.89 v.u., suggesting that the Mn3 site is likely to be occupied roughly equally by Mn and Fe. Based on the BVS values for the other Mn sites, 2.06 v.u. for Mn1, 1.99 v.u. for Mn2 and 2.07 v.u. for Mn4, we suggest that the 0.87 Fe apfu provided by the EPMA could be allocated as follows: Mn1: $Mn_{0.80}Fe_{0.20}$ (BVS = 2.02 v.u.), Mn2: $Mn_{1.00}Fe_{0.00}$ (BVS = 1.99 v.u.), Mn3: $Mn_{0.55}Fe_{0.45}$ (BVS = 2.02 v.u.), and Mn4: $Mn_{0.78}Fe_{0.22}$ (BVS = 2.02 v.u.). Nevertheless, the best refinement was obtained with all four Mn sites assigned full occupancies by Mn only.

Atomic arrangement

The structure of jasonsmithite (Figs. 5 and 6) contains zigzag chains of edge-sharing MnO_6 octahedra along [100]. The chains are linked into sheets parallel to {001} by sharing corners

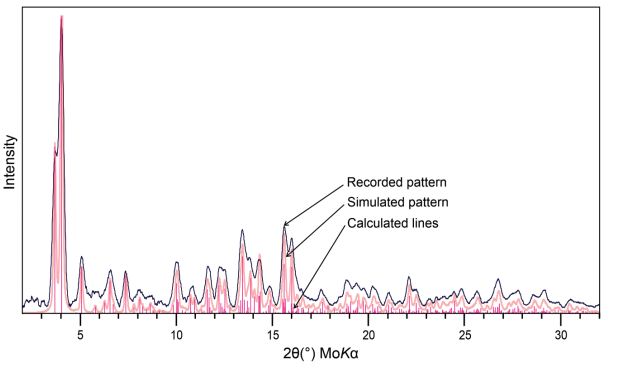

Figure 4. The observed powder diffraction pattern compared with the pattern simulated from the lines calculated from the crystal structure. (Color online.)

Table 2. Selected bond distances (Å) for jasonsmithite

Mn1-O12	2.117(4)	Mn4-O2	2.084(4)	P1-O1	1.515(4)
Mn1-O1	2.130(3)	Mn4-O7	2.122(3)	P1-O2	1.519(4)
Mn1-O15	2.131(4)	Mn4-O16	2.161(3)	P1-O3	1.551(3)
Mn1-O7	2.170(3)	Mn4-O11	2.177(3)	P1-O4	1.571(4)
Mn1-OW21	2.214(4)	Mn4-OW24	2.270(4)	<P1-O>	1.539
Mn1-OW22	2.423(4)	Mn4-OW22	2.350(4)		
<Mn1-O>	2.198	<Mn4-O>	2.194	P2-O5	1.510(4)
				P2-O6	1.528(4)
Mn2-O3	2.114(3)	Zn-O13	1.922(4)	P2-O7	1.533(3)
Mn2-O6	2.125(4)	Zn-O4	1.978(3)	P2-O8	1.554(3)
Mn2-O11	2.139(3)	Zn-OW18	1.990(4)	<P2-O>	1.531
Mn2-O16	2.175(3)	Zn-O8	1.990(4)		
Mn2-OW21	2.279(4)	<Zn-O>	1.970	P3-O9	1.517(4)
Mn2-OW23	2.470(4)			P3-O10	1.535(4)
<Mn2-O>	2.217	Al-O9	1.829(4)	P3-O11	1.542(3)
		Al-O5	1.845(4)	P3-O12	1.543(4)
Mn3-O12	2.117(4)	Al-OH17	1.899(4)	<P3-O>	1.534
Mn3-O3	2.160(3)	Al-OW20	1.936(4)		
Mn3-O8	2.165(3)	Al-OW19	1.940(4)	P4-O13	1.542(4)
Mn3-O15	2.189(4)	Al-OH17	1.941(4)	P4-O14	1.542(4)
Mn3-OW23	2.193(4)	<Al-O>	1.898	P4-O15	1.543(4)
Mn3-OW24	2.228(4)			P4-O16	1.543(3)
<Mn3-O>	2.175			<P4-O>	1.543

Hydrogen bonds

D–H···*A*	*D*–H	H···*A*	*D*···*A*	<*DHA*
OH17-H17···O1	0.81(3)	1.99(3)	2.799(5)	171(6)
OW18-H18A···OH17	0.85(3)	1.89(3)	2.731(5)	172(6)
OW18-H18B···OW25	0.81(3)	2.24(4)	2.911(8)	141(6)
OW19-H19A···O4	0.82(3)	1.92(3)	2.730(5)	167(5)
OW19-H19B···O4	0.81(3)	1.84(3)	2.644(5)	172(6)
OW20-H20A···O6	0.84(3)	1.85(3)	2.685(5)	170(6)
OW20-H20B···OW26	0.78(3)	1.96(3)	2.735(7)	176(7)
OW21-H21A···O14	0.84(3)	1.90(3)	2.706(5)	161(5)
OW21-H21B···O10	0.82(3)	1.85(3)	2.641(5)	164(5)
OW22-H22A···OW27	0.83(3)	1.98(3)	2.801(16)	170(6)
OW22-H22A···OW28	0.83(3)	1.91(4)	2.715(15)	163(5)
OW22-H22B···O6	0.82(3)	2.23(3)	3.043(5)	168(6)
OW23-H23A···O2	0.82(3)	1.89(3)	2.703(5)	171(6)
OW23-H23B···OW25	0.82(3)	1.89(3)	2.695(7)	166(6)
OW24-H24A···O10	0.83(3)	1.95(3)	2.709(5)	153(5)
OW24-H24B···O14	0.81(3)	1.85(3)	2.602(5)	154(6)
OW25-H25B···OW26	0.84(3)	2.52(4)	3.304(11)	156(8)
OW25-H25B···OW29	0.84(3)	2.33(7)	2.908(15)	126(7)
OW26-H26A···O10	0.83(3)	1.86(3)	2.677(7)	167(10)
OW26-H26B···OW27	0.84(3)	2.36(8)	2.976(16)	131(8)
OW26-H26B···OW29	0.84(3)	2.25(6)	3.005(15)	150(10)

Table 3. Bond-valence analysis for jasonsmithite

	Mn1	Mn2	Mn3	Mn4	Al	Zn	P1	P2	P3	P4	Hydrogen bonds	sum
O1	0.39						1.31				0.18	1.89
O2				0.44			1.30					1.74
O3		0.41	0.37				1.20					1.97
O4						0.46	1.14				0.21, 0.26	2.08
O5					0.58			1.33				1.91
O6		0.40						1.27			0.23, 0.12	2.02
O7	0.36			0.40				1.26				2.01
O8			0.36			0.45		1.19				2.00
O9					0.61				1.31			1.91
O10									1.25		0.24, 0.26, 0.22	1.97
O11		0.38		0.35					1.23			1.96
O12	0.40		0.40						1.23			2.03
O13						0.54				1.23		1.77
O14										1.23	0.22, 0.29	1.74
O15	0.39		0.34							1.23		1.96
O16		0.35		0.36						1.23		1.94
OH17					0.51						−0.18, 0.21	1.00
					0.46							
OW18						0.45					−0.21, −0.15	0.09
OW19					0.46						−0.21, −0.26	−0.01
OW20					0.46						−0.23, −0.21	0.01
OW21	0.32	0.27									−0.22, −0.26	0.11
OW22	0.19			0.23							−0.22, −0.12	0.08
OW23		0.17	0.34								−0.23, −0.23	0.06
OW24			0.31	0.28							−0.22, −0.29	0.08
OW25											−0.09, −0.15, 0.15	−0.09
OW26											−0.24, 0.21, 0.09	0.06
sum	2.06	1.99	2.12	2.07	3.07	1.90	4.96	5.05	5.01	4.91		

Notes: Values are expressed in valence units. Bond-valence parameters are from Gagné and Hawthorne (2015). Hydrogen-bond strengths based on O-O bond lengths from Ferraris and Ivaldi (1988). Half-occupied OW27, OW28, and OW29 sites are not included.

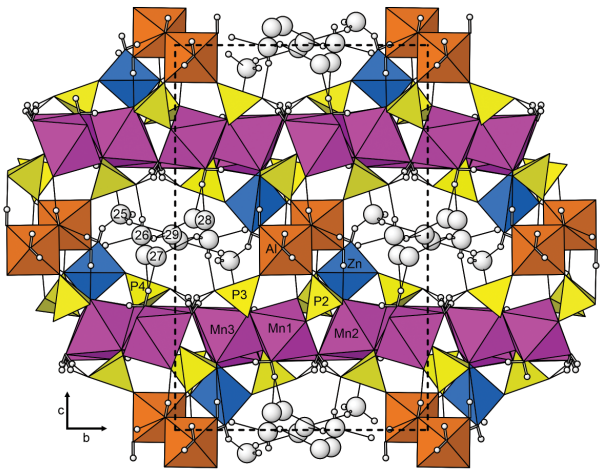

Figure 5. Crystal structure of jasonsmithite viewed down **a**. The O atoms of the channel H_2O groups (OW25, OW26, OW27, OW28, and OW29) are numbered. (Color online.)

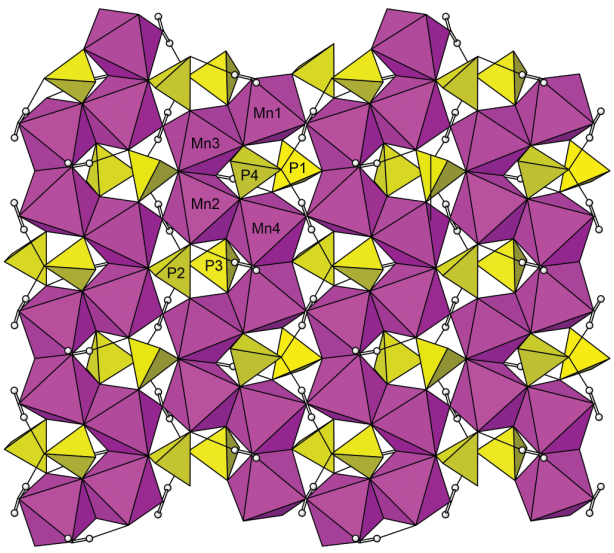

Figure 6. The sheet of octahedra and tetrahedra in the jasonsmithite structure viewed down **c*** with **a** vertical and **b** horizontal. Except for minor geometric deviations, this sheet is identical to those in angarfite, bakhchisaraitsevite, and mejillonesite. (Color online.)

with octahedra in adjacent chains and by sharing corners with peripheral PO_4 tetrahedra. A ZnO_4 tetrahedron decorates the sheet, sharing three of its corners with polyhedra in the sheet; its unshared fourth corner is an H_2O group. Dimers of edge-sharing AlO_6 octahedra corner-link to PO_4 tetrahedra in adjacent sheets, thereby linking the sheets into a framework. The framework contains large channels along [100] that contain five different H_2O sites (OW25, OW26, OW27, OW28, and OW29). OW25 and OW26 are fully occupied. OW27 and OW28 are only 0.710(16) Å apart and OW29 is only 1.65(2) Å from an equivalent OW29 site across the 0,0,½ center of symmetry. These three sites refined to close to half occupancy and were assigned half occupancies in the final refinements. The OW27, OW28, and OW29 sites were the only H_2O O sites for which the associated H sites could not be located.

While the structure of jasonsmithite is unique among natural and synthetic phases, the sheet of octahedra and tetrahedra that it contains (Fig. 6) is topologically identical to those in angarfite, $NaFe_5^{3+}(PO_4)_4(OH)_4(H_2O)_4$ (Kampf et al. 2012), bakhchisaraitsevite, $Na_2Mg_5(PO_4)_4(H_2O)_6 \cdot H_2O$ (Liferovich et al. 2000; Yakubovich et al. 2000), liversidgeite, $Zn_6(PO_4)_4(H_2O)_5 \cdot 2H_2O$ (Elliott et al. 2010), mejillonesite, $NaMg_2(PO_3OH)(PO_4)(OH)(H_5O_2)$ (Atencio et al. 2012), and rimkorolgite, $BaMg_5(PO_4)_4(H_2O)_7 \cdot H_2O$ (Krivovichev et al. 2002). The manner in which these sheets are linked to one another differs for each of these minerals.

Implications

The structure of jasonsmithite contains 1D channels that are contained within 14-member rings (14MR) comprised of six MnO_6 octahedra, four AlO_6 octahedra, and four PO_4 tetrahedra (Fig. 7), which define a high-porosity framework with the potential for high molecular conductivity. The 14MR are oriented parallel to the {103} plane that creates a pillared-like geometry to support the Mn-sheets (cf. Clearfield and Wang 2002). The channels have side-branch pockets containing extra-framework H_2O that are similar to other interrupted microporous frameworks [e.g., scandium phosphates (Bull et al. 2003; Park et al. 2004)]. Calculated void space (with extra-framework H_2O removed) using the CrystalMaker software yielded a void space of 70.2% per unit cell, and a framework density of 14.5 polyhedral atoms/1000 Å^3, which would place it among the most porous minerals as compared to zeolites (Baerlocher et al. 2007). The largest cavity is located at 0,½,0 with a diameter of 6.4 Å. The tetrahedrally coordinated P atoms at sites P3 and P4 each have one oxygen (O10 and O14, respectively) that does not bridge directly to another framework cation. Sites O10 and O14 form hydrogen bonds to the extra-framework H_2O in the channels. Framework Zn in microporous structures has been previously found to show promising catalytic activity (Orazov and Davis 2016). The presence of a hydrated Zn polyhedron along the walls of the jasonsmithite channels may provide a site for catalytic activity if hydrolyzed to form a Lewis acid center, and this would be worth further exploration in the search of low-temperature microporous catalysts. The solvent-accessible void space is shown in Figure 8.

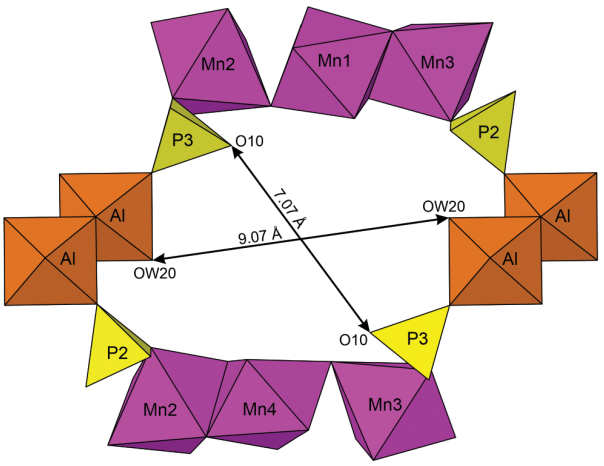

Figure 7. The 14-member ring (14MR) in the structure of jasonsmithite viewed along **a**.

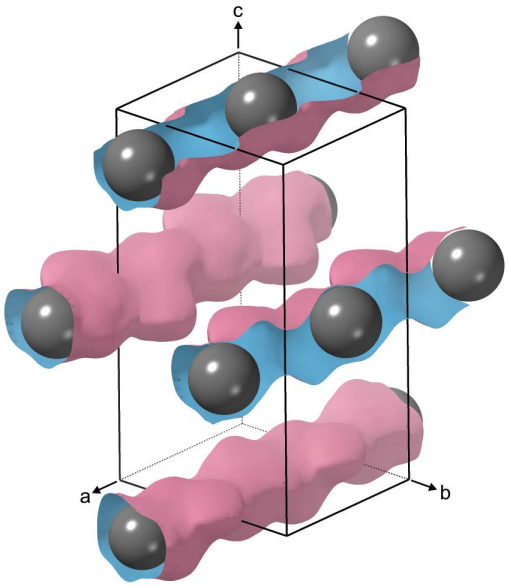

Figure 8. Map of calculated solvent-accessible void space to a distance of 1.2 Å from the nearest van der Waals surface. Blue shows inner surface of channel. Gray spheres show areas of largest cage volume. The unit-cell outline is shown. (Color online.)

Acknowledgments

Reviewers Ian Grey and Fernando Colombo are thanked for their constructive comments on the manuscript. A portion of this study was funded by the John Jago Trelawney Endowment to the Mineral Sciences Department of the Natural History Museum of Los Angeles County.

References cited

Atencio, D., Chukanov, N.V., Nestola, F., Witzke, T., Coutinho, J.M.V., Zadov, A.E., Contreira Filho, R.R., and Färber, G. (2012) Mejillonesite, a new acid sodium, magnesium hydrogen phosphate mineral from Mejillones, Antofagasta, Chile. American Mineralogist, 97, 19–25.

Baerlocher, C., McCusker, L.B., and Olson, D.H. (2007) Atlas of zeolite framework types. Elsevier.

Bull, I., Young, V., Teat, S.J., Peng, L., Grey, C.P., and Parise, J.B. (2003) Hydrothermal synthesis and structural characterization of four scandium phosphate frameworks. Chemistry of Materials, 15, 3818–3825.

Clearfield, A., and Wang, Z. (2002) Organically pillared microporous zirconium phosphonates. Journal of the Chemical Society, Dalton Transactions, 15,

2937–2947.
Elliott, P., Giester, G., Libowitzky, E., and Kolitsch, U. (2010) Description and crystal structure of liversidgeite, $Zn_6(PO_4)_4 \cdot 7H_2O$, a new mineral from Broken Hill, New South Wales, Australia. American Mineralogist, 95, 397–404.
Ferraris, G., and Ivaldi, G. (1988) Bond valence vs. bond length in O···O hydrogen bonds. Acta Crystallographica, B44, 341–344.
Gagné, O.C., and Hawthorne, F.C. (2015) Comprehensive derivation of bond-valence parameters for ion pairs involving oxygen. Acta Crystallographica, B71, 562–578.
Higashi, T. (2001) ABSCOR. Rigaku Corporation, Tokyo.
Kampf, A.R., Mills, S.J., Housley, R.M., Boulliard, J.-C., and Bourgoin, V. (2012) Angarfite, $NaFe^{3+}_5(PO_4)_4(OH)_4 \cdot 4H_2O$, a new mineral from the Angarf-Sud pegmatite, Morocco: Description and crystal structure. Canadian Mineralogist, 50, 781–791.
Krivovichev, S.V., Britvin, S.N., Burns, P.C., and Yakovenchuk, V.N. (2002) Crystal structure of rimkorolgite, $Ba[Mg_5(H_2O)_7(PO_4)_4](H_2O)$, and its comparison with bakhchisaraitsevite. European Journal of Mineralogy, 14, 397–402.
Liferovich, R.P., Pakhomovsky, Y.A., Yakubovich, O.V., Massa, W., Laajoki, K., Gehör, S., Bogdanova, A.N., and Sorokhtina, N.V. (2000) Bakhchisaraitsevite, $Na_2Mg_5[PO_4]_4 \cdot 7H_2O$, a new mineral from hydrothermal assemblages related to phoscorite-carbonatite complex of the Kovdor massif, Russia. Neues Jahrbuch für Mineralogie, Monatshefte, 402–418.
Mandarino, J.A. (2007) The Gladstone-Dale compatibility of minerals and its use in selecting mineral species for further study. Canadian Mineralogist, 45, 1307–1324.
Orazov, M., and Davis, M.E. (2016) Catalysis by framework zinc in silica-based molecular sieves. Chemical Science, 7, 2264–2274.
Park, H., Bull, I., Peng, L., Young, V.G., Grey, C.P., and Parise, J.B. (2004) Synthesis and structure determination of a new organically templated scandium fluorophosphate framework and its indium analogue. Chemistry of Materials, 16, 5350–5356.
Pouchou, J.-L., and Pichoir, F. (1991) Quantitative analysis of homogeneous or stratified microvolumes applying the model "PAP." In K.F.J. Heinrich and D.E. Newbury, Eds., Electron Probe Quantitation. Plenum Press, pp. 3l–75.
Rakovan, J., Barnett, B., and White, J.S. (2016) Fluorapatite from the Foote mine, Kings Mountain, North Carolina. Rocks and Minerals, 91, 251–256.
Sheldrick, G.M. (2015a) SHELXT—Integrated space-group and crystal-structure determination. Acta Crystallographica, A71, 3–8.
——— (2015b) Crystal structure refinement with SHELX. Acta Crystallographica, C71, 3–8.
Yakubovich, O.V., Massa, W., Liferovich, R.P., and Pakhomovsky, Y.A. (2000) The crystal structure of bakhchisaraitsevite, $[Na_2(H_2O)_2]\{(Mg_{4.5}Fe_{0.5})(PO_4)_4(H_2O)_5\}$, a new mineral species of hydrothermal origin from the Kovdor phoscorite-carbonatite complex, Russia. Canadian Mineralogist, 38, 831–838.

Manuscript received May 1, 2020
Manuscript accepted June 29, 2020
Manuscript handled by G. Diego Gatta

Endnote:

[1]Deposit item AM-21-27582, CIF and Online Material. Deposit items are free to all readers and found on the MSA website, via the specific issue's Table of Contents (go to http://www.minsocam.org/MSA/AmMin/TOC/2021/Feb2021_data/Feb2021_data.html). The CIF has been peer-reviewed by our Technical Editors.